ADVANCED FUNCTIONAL MATERIALS
www.afm-journal.de

Materials Views
www.MaterialsViews.com

Colossal Thermoelectric Power Factor in $K_{7/8}RhO_2$

*Yasir Saeed, Nirpendra Singh, and Udo Schwingenschlögl**

The thermoelectric properties of the layered oxides K_xRhO_2 ($x = 1/2$ and 7/8) are investigated by means of the electronic structure, as determined by ab inito calculations and Boltzmann transport theory. In general, the electronic structure of K_xRhO_2 is similar to Na_xCoO_2, but with strongly enhanced transport. $K_{7/8}RhO_2$ exceeds the ultrahigh power factor of $Na_{0.88}CoO_2$ reported previously by more than 50%. The roles of the cation concentration and the lattice parameters in the transport properties in this class of compounds are explained.

1. Introduction

Thermoelectric materials, which convert heat into electric power, are of growing interest for energy conversion. A number of promising classes of materials have been identified: bismuth tellurids,[1–4] III-nitrides (AlInN and InGaN),[5–9] SiGe alloys,[10,11] and oxides.[12] Due to their stability against oxidation, oxides are most suitable for power generation from waste heat at high temperature (in air). Layered cobalt oxides have received special attention.[12–16] By varying the Na concentration in Na_xCoO_2 the system changes its behavior from metallic to insulating and becomes superconducting around $x = 0.3$.[14,15] A strong enhancement of the thermopower in Na_xCoO_2 has been observed for high Na doping.[16] A peak value of the Seebeck coefficient of 250 μV K^{-1} at 125 K is among the highest values for hole-type materials. Recently, the room temperature Seebeck coefficient of Na_xCoO_2 was reported to fall in the range from 30 to 100 μV K^{-1}[17] and to increase with increasing Na concentration. Although the values are smaller than claimed in Lee et al.,[16] the materials are still very interesting for application in thermoelectrics. This fact has promoted huge interest in the isostructural and isovalent families A_xCoO_2, A = K, Rb, or Cs. Angle-resolved photoemission spectroscopy points to similar electronic and optical properties of $K_{1/2}CoO_2$ and $Na_{1/2}CoO_2$, which has been confirmed by band structure calculations.[18–21] The electronic structure of Na_xCoO_2 is discussed by Johannes and Singh.[22]

Analogous compounds with Rh in place of Co are found to be good thermoelectric materials, but with reduced correlation effects.[21,23–26] Shibasaki et al.[27] have shown that the substitution of Rh ions in $La_{0.8}Sr_{0.2}Co_{1-x}Rh_xO_{3-\delta}$ diminishes the magnetic moment of Co, where the thermopower is enhanced by a factor of 10 at $x = 1/2$ as compared to $x = 0$ and $x = 1$. The optical and thermoelectric properties of $K_{0.49}RhO_2$ have been investigated by Okazaki et al.[28,29] who report on qualitative similarities of the optical conductivity spectra as compared to Na_xCoO_2. An experimental Seebeck coefficient of 40 μV K^{-1} (at 300 K) is found.[28] The temperature dependence of the transport is different from Na_xCoO_2, which also suggests that correlations are weaker in the Rh oxides than in the Co oxides. An enhancement of the transport for an increasing concentration of alkali cations is known from other layered oxides.[30] Despite various studies, the electronic structure of the 4d systems is not well understood.[31,32] Still, Rh and Co are similar from a chemical point of view so that layered Rh oxides can be synthesized with properties largely resembling those of the Co oxides.[33–35]

We propose a new class of materials with enhanced thermoelectric power factor employing first principles calculations for K_xRhO_2 with $x = 1/2$ and 7/8. A comparison to Na_xCoO_2 is given in terms of the chemical nature of the Co 3d and Rh 4d states. The optical transitions are explained by the band structure (BS) and density of states (DOS), and the influence of the cation concentration as well as the lattice parameters on the power factor, which is key for thermoelectric devices, is discussed.

2. Computational Details

Our calculations are based on density functional theory using the full-potential linearized augmented plane wave approach as implemented in the WIEN2k package.[36] This method has been applied successfully in many cases for describing the electronic structure of oxides,[37,38] including the optical spectrum.[39] The transport is calculated by semiclassical Boltzmann theory in the constant scattering approximation, implemented in the BoltzTraP code.[40,41] Different exchange-correlation functionals (local density approximation (LDA), generalized gradient approximation (GGA), GGA-sol, and GGA-PBE0) are employed in the optimization of the c/a ratio. Since the differences are small, we will discuss in the following only the GGA-sol results.

In our calculations the unit cell is divided into non-overlapping atomic spheres, centered at the atomic sites, and the interstitial region. The parameter $R_{mt}K_{max}$ (where K_{max} is the plane-wave cut-off and R_{mt} is the smallest muffin-tin radius) controls the size of the basis. It is set to a high value of 7 together with $G_{max} = 24$. We use 66 **k**-points in the irreducible wedge of the Brillouin zone for calculating the electronic structure and

Y. Saeed, Dr. N. Singh, Prof. U. Schwingenschlögl
PSE Division, KAUST, Thuwal 23955-6900
Kingdom of Saudi Arabia
E-mail: udo.schwingenschlogl@kaust.edu.sa

DOI: 10.1002/adfm.201103106

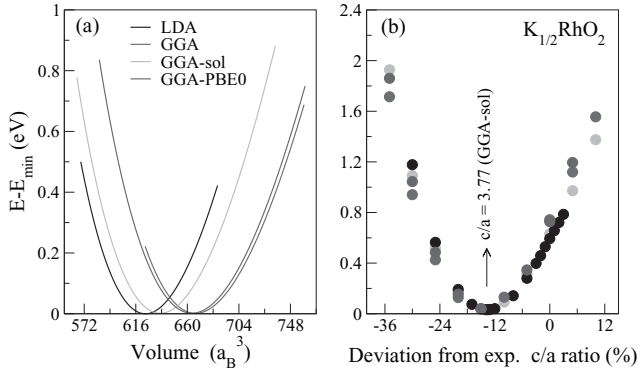

Figure 1. Volume optimization of $K_{1/2}RhO_2$ for different exchange correlation functionals.

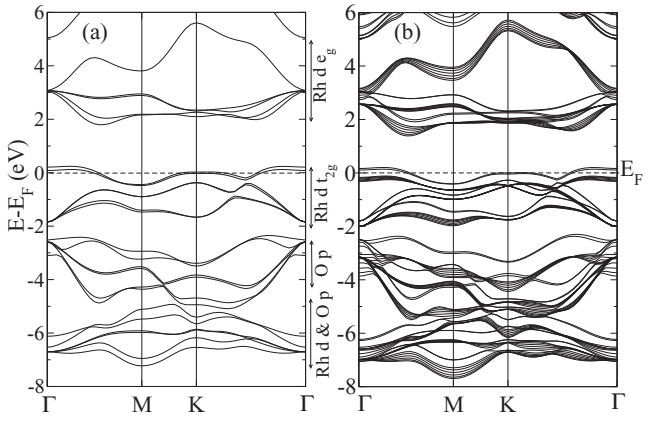

Figure 2. Energy band structures of: a) $K_{1/2}RhO_2$ and b) $K_{7/8}RhO_2$.

a dense mesh of 480 **k**-points in the optical calculations. For the transport calculations we apply 4592 **k**-points. Self-consistency is assumed to be achieved for a total energy convergence of 10^{-5} Ry.

3. Results and Discussion

K_xRhO_2 crystallizes in the γ-Na_xCoO_2 structure with space group $P6_3/mmc$ and experimental lattice constants of $a = 3.0647$ Å and $c = 13.6$ Å.[42] The CdI_2-type RhO_2 layer and the K layer are stacked alternately along the *c*-axis. The experimental lattice constants of $K_{1/2}RhO_2$ are used as starting point for the structure optimization, yielding the volume and *c*/*a* ratio presented in **Figure 1**. Our LDA calculation yields an approximately 14% reduction of the *c*/*a* ratio from 4.44 (experimental) to 3.84 (optimized), which is similar to other layered Co/Rh oxides (*c*/*a* ≈ 3.8). The Rh–O bond length is reduced from 2.13 to 2.04 Å. To confirm the result, we have optimized the structure with more involved exchange correlation functionals (GGA, GGA-sol, and PBE0), but obtain almost the same in each case. In addition, the optimized lattice parameters lead to a good agreement of the optical and transport properties with the experiment (details below).

The optimized *c* value is also similar to other isostructural compounds such as Sr_xRhO_2,[43,44] Na_xCoO_2,[19] Li_xNbO_2,[45] and La_xCoO_2.[46] Interestingly, the layered materials $LiRhO_2$, $NaRhO_2$, and $KRhO_2$ can form hydrate (i.e., water intercalated) phases[31] with increased *c* lattice parameter.[47] Takada et al.[14] have shown that Na_xCoO_2 can be readily hydrated to form $Na_xCoO_2 \cdot yH_2O$. The *c* lattice parameter again is considerably expanded to accomodate the intercalated water. We therefore conjecture that the experimental structure of K_xRhO_2 refers to the hydrated phase while the optimized lattice constants $a = 3.06$ and $c = 11.56$ Å represent the ideal structure. We first focus on the optimized lattice constants.

In **Figure 2**a,b the calculated electronic BSs of $K_{1/2}RhO_2$ and $K_{7/8}RhO_2$ are presented. They are similar to isostructural and isovalent Na_xCoO_2, except for a slightly larger pseudogap between the Rh t_{2g} and e_g bands. The less dispersive bands in K_xRhO_2 as compared to Na_xCoO_2 promote an enhanced thermoelectricity. The DOS in **Figure 3** reflects the crystal field splitting into e_g and t_{2g} states experienced by the Rh^{4+} ions, similar to Na_xCoO_2 but with larger bandwidths.[29] The increased bandwidths reflect a reduction of the electronic correlations. In addition, a weak hybridization between the Rh 4d and O 2p states is seen in the DOS at or below the Fermi energy, and the O 2p states lie deeper in the valence band (below –2 eV) than in Na_xCoO_2.

The optical reflectivity and conductivity of K_xRhO_2 are shown in **Figure 4**a,b, where the experimental values are taken from Okazaki et al.[29] The calculated reflectivities are similar to each other, with a maximum value of approximately 90% at zero photon energy. A Drude-like edge is found at around 1 eV (experiment: 1.2 eV) in the reflectivity spectrum of $K_{1/2}RhO_2$, while for $K_{7/8}RhO_2$ this edge appears at around 0.5 eV. At zero photon energy, the calculated optical conductivity of $\sigma \approx 2500\ \Omega^{-1}\ cm^{-1}$ for $K_{1/2}RhO_2$ is in excellent agreement with the experiment, see the blue and black dots in Figure 4b. Three well-defined peaks are observed: i) near 1 eV due to the Rh t_{2g}–t_{2g} intra-band transition, ii) at around 3 eV due to the Rh t_{2g}–e_g inter-band transition, and iii) around 5.5 eV due to the inter-band transition from O 2p to Rh 4d e_g. The peaks are also present in the experiment,[29] as well as for $Na_{1/2}CoO_2$ (0.5 eV, 1.6 eV, and 3 eV),[18] which again reflects the similarity of these isostructural and isovalent compounds.

In the following, we will address the experimental (hydrated) as well as optimized structures of K_xRhO_2. We have calculated

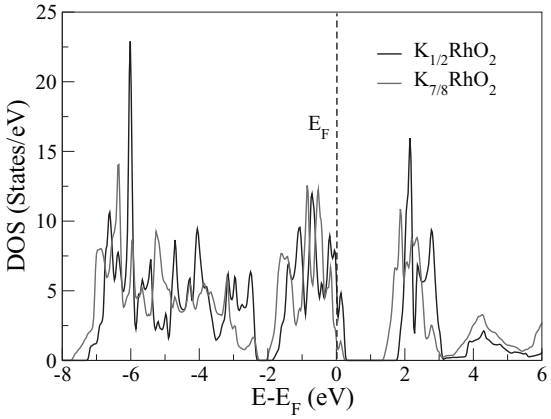

Figure 3. DOS obtained for $K_{1/2}RhO_2$ and $K_{7/8}RhO_2$.

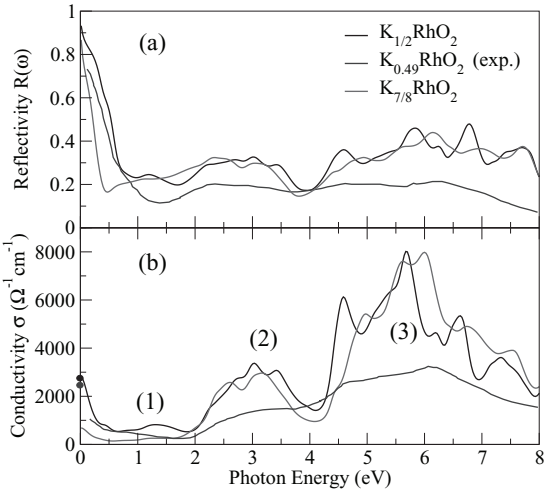

Figure 4. Optical reflectivity and conductivity of $K_{1/2}RhO_2$ and $K_{7/8}RhO_2$ along with experimental spectra.[29] Blue and black dots highlight the calculated and experimental values at zero photon energy.

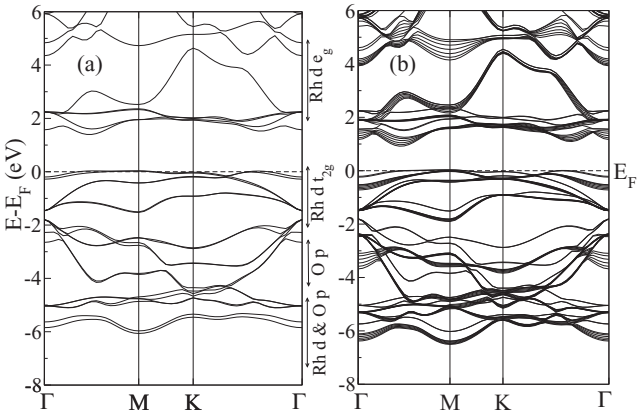

Figure 6. Energy band structures of hydrated a) $K_{1/2}RhO_2$ and b) $K_{7/8}RhO_2$.

the Seebeck coefficient (S), thermal conductivity (κ), and power factor (Z). The data are shown in **Figure 5** as a function of the temperature from 0 to 700 K. According to Figure 5 a, at 300 K the Seebeck coefficients of optimized $K_{1/2}RhO_2$ and $K_{7/8}RhO_2$ amount to 50 and 55 μV K^{-1}, respectively, in good agreement with the experiment.[28] For hydrated $K_{1/2}RhO_2$ and $K_{7/8}RhO_2$, on the other hand, the values are strongly enhanced to 100 and 140 μV K^{-1}, respectively.

The BS of the hydrated phase of K_xRhO_2 is close to that of optimized K_xRhO_2, compare Figure 2 and **Figure 6**, except that the Rh t_{2g} bands are flatter in a narrow region around the Fermi energy. This fact causes the resistivity to increase and results in a higher Seebeck coefficient. The larger S value for $K_{7/8}RhO_2$ as compared to $K_{1/2}RhO_2$ is due to band filling by the increased cation concentration, which (rigidly) shifts flatter regions of the bands towards the Fermi energy. For comparison, we have calculated the room temperature Seebeck coefficient of $Na_{1/2}CoO_2$ for the lattice parameters: i) a = 2.88 Å, c = 15.59 Å[48] and ii) a = 2.86 Å, c = 10.82 Å. We obtain 60 and 34 μV K^{-1}, respectively, which is in agreement with the experiment[17] and seconds the above picture that a larger c parameter can enhance S. We finally have to address the question why hydrated K_xRhO_2 has a higher Seebeck coefficient than hydrated Na_xCoO_2. According to the BS given in **Figure 7**, the larger c lattice parameter of Na_xCoO_2 (15.59 Å as compared to 13.6 Å) causes the Co e_g states to shift down in energy to the Fermi level because the Co–O overlap is reduced. This, in turn, results in a decrease of the resistivity and, therefore, the Seebeck coefficient. Note that the carrier concentrations are 1.0×10^{21} cm^{-3} in hydrated $Na_{1/2}CoO_2$ and 1.8×10^{21} cm^{-3} in hydrated $K_{1/2}RhO_2$.

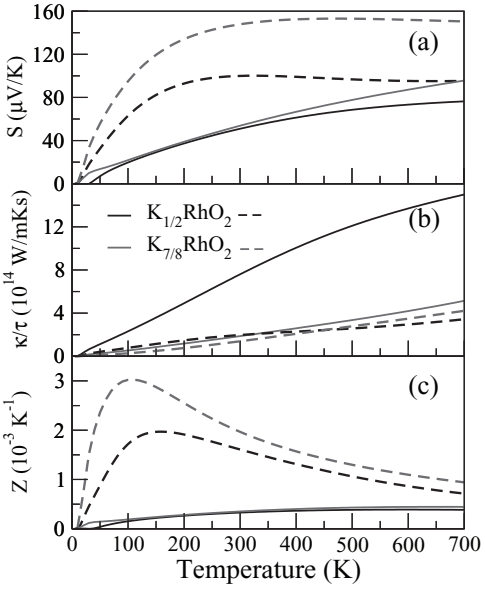

Figure 5. Calculated thermoelectric properties of pristine (solid line) and hydrated (dashed line) K_xRhO_2.

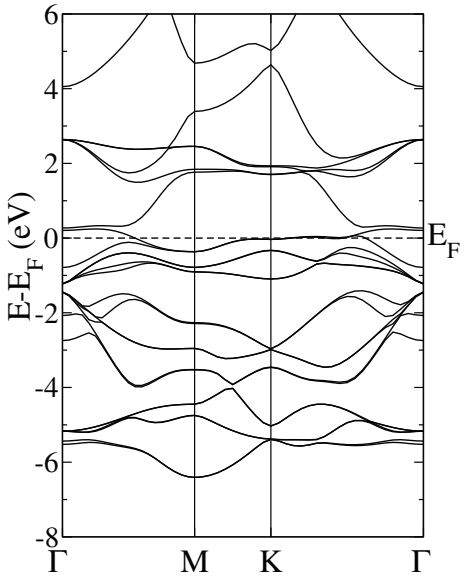

Figure 7. Energy band structure of $Na_{1/2}CoO_2$ with c = 15.59 Å.

For optimized K_xRhO_2 the Seebeck coefficient depends not much on the K concentration up to 300 K, whereas for higher temperatures it increases stronger for $K_{7/8}RhO_2$ to reach a value of 80 μV K^{-1} at 700 K. In contrast to this behavior, *S* remains almost constant above 300 K for hydrated K_xRhO_2. According to Figure 5 b the thermal conductivity is similar for the hydrated phases and for optimized $K_{7/8}RhO_2$, while it is much enhanced for optimized $K_{1/2}RhO_2$. In Figure 5 c, the power factor is presented for optimized and hydrated K_xRhO_2. For hydrated $K_{7/8}RhO_2$ it reaches a value of 3×10^{-3} K^{-1} at 100 K. This is much higher than in other hole-type compounds, including $Na_{0.88}CoO_2$ with a maximum of $Z = 1.8 \times 10^{-3}$ K^{-1} (at 80 K). At room temperature (300 K) the power factor of hydrated K_xRhO_2 also clearly exceeds that of $Na_{0.88}CoO_2$, whereas for optimized K_xRhO_2 it is only a little higher. The large *Z* of hydrated K_xRhO_2 results from a decrease of the thermal conductivity, increase of the electrical conductivity (as demonstrated for the hydrated phase of $NaRhO_2$ in Figure 2 of Park et al.[47]), and larger Seebeck coefficient as compared to optimized K_xRhO_2.

4. Conclusion

In conclusion, the electronic, optical, and transport properties of the layered compounds K_xRhO_2 have been determined and compared to isostructural and isovalent Na_xCoO_2. The optimized structure of $K_{1/2}RhO_2$ exhibits a remarkable deviation of the *c*/*a* ratio from the experimental result as well as from *c*/*a* ratios of related compounds. This indicates that a hydrated phase of K_xRhO_2 exists and that the experimental structure determination refers to this hydrated phase. The calculated Seebeck coefficient of pristine $K_{1/2}RhO_2$ amounts to 50 μV K^{-1} at 300 K, which is close to the experimental value of 40 μV K^{-1}. Importantly, we find huge values for the Seebeck coefficient and power factor for hydrated K_xRhO_2 in the whole temperature range from 0 to 700 K. At 100 K, we obtain for hydrated $K_{7/8}RhO_2$ a value of $Z = 3 \times 10^{-3}$ K^{-1}, which is the highest power factor observed at this temperature. It exceeds the exceptionally high value of $Na_{0.88}CoO_2$ by more than 50%. Our results demonstrate that hydration is an effective approach to modify the lattice parameters and, as a result, enhance the thermoelectric performance. The transport properties of K_xRhO_2 are highly promising for technological applications.

Received: December 21, 2011
Revised: February 10, 2012
Published online: April 12, 2012

[1] G. Chen, A. Shakouri, *J. Heat Transfer* **2002**, *124*, 242.
[2] G. Chen, M. S. Dresselhaus, J.-P. Fleurial, T. Caillat, *Int. Mater. Rev.* **2003**, *48*, 45.
[3] B. Poudel, Q. Hao, Y. Ma, Y. Lan, A. Minnich, B. Yu, X. Yan, D. Wang, A. Muto, D. Vashaee, X. Chen, J. Liu, M. S. Dresselhaus, G. Chen, Z. Ren, *Science* **2008**, *320*, 634.
[4] Y. Lan, B. Poudel, Y. Ma, D. Wang, M. S. Dresselhaus, G. Chen, Z. F. Ren, *Nano Lett.* **2009**, *9*, 1419.
[5] H. Tong, J. Zhang, G. Liu, J. A. Herbsommer, G. S. Huang, N. Tansu, *Appl. Phys. Lett.* **2010**, *97*, 112105.
[6] J. Zhang, H. Tong, G. Liu, J. A. Herbsommer, G. S. Huang, N. Tansu, *J. Appl. Phys.* **2011**, *109*, 053706.
[7] J. Zhang, S. Kutlu, G. Liu, N. Tansu, *J. Appl. Phys.* **2011**, *110*, 043710.
[8] A. Sztein, H. Ohta, J. E. Bowers, S. P. DenBaars, S. Nakamura, *J. Appl. Phys.* **2011**, *110*, 123709.
[9] B. N. Pantha, I. Feng, K. Aryal, J. Li, J. Y. Lin, H. X. Jiang, *Appl. Phys. Express* **2011**, *4*, 051001.
[10] S. K. Bux, R. G. Blair, P. K. Gogna, H. Lee, G. Chen, M. S. Dresselhaus, R. B. Kaner, J. P. Fleurial, *Adv. Funct. Mater.* **2009**, *19*, 2445.
[11] C. Hin, M. Dresselhaus, G. Chen, *Appl. Phys. Lett.* **2010**, *97*, 251909.
[12] I. Terasaki, Y. Sasago, K. Uchinokura, *Phys. Rev. B* **1997**, *56*, R12685.
[13] T. Motohashi, R. Ueda, E. Naujalis, T. Tojo, I. Terasaki, T. Atake, M. Karppinen, H. Yamauchi, *Phys. Rev. B* **2003**, *67*, 064406.
[14] K. Takada, H. Sakurai, E. Takayama-Muromachi, F. Izumi, R. A. Dilanian, T. Sasaki, *Nature* **2003**, *422*, 53.
[15] M. L. Foo, Y. Wang, S. Watauchi, H. W. Zandbergen, T. He, R. J. Cava, N. P. Ong, *Phys. Rev. Lett.* **2004**, *92*, 247001.
[16] M. Lee, L. Viciu, L. Li, Y. Wang, M. L. Foo, S. Watauchi, R. A. Pascal, R. J. Cava, N. P. Ong, *Nat. Mater.* **2006**, *5*, 537.
[17] N. Kaurav, K. K. Wu, Y. K. Kuo, G. J. Shu, F. C. Chou, *Phys. Rev. B* **2009**, *79*, 075105.
[18] M. D. Johannes, I. I. Mazin, D. J. Singh, *Phys. Rev. B* **2005**, *71*, 205103.
[19] J. Sugiyama, H. Nozaki, Y. Ikedo, K. Mukai, J. H. Brewer, E. J. Ansaldo, G. D. Morris, D. Andreica, A. Amato, T. Fujii, A. Asamitsu, *Phys. Rev. Lett.* **2006**, *96*, 037206.
[20] J. Sugiyama, Y. Ikedo, P. L. Russo, H. Nozaki, K. Mukai, D. Andreica, A. Amato, M. Blangero, C. Delmas, *Phys. Rev. B* **2007**, *76*, 104412.
[21] K. W. Lee, W. E. Pickett, *Phys. Rev. B* **2007**, *76*, 134510.
[22] M. D. Johannes, D. J. Singh, *Phys. Rev. B* **2004**, *70*, 014507.
[23] W. Koshibae, K. Tsutsui, S. Maekawa, *Phys. Rev. B* **2000**, *62*, 6869.
[24] Y. Klein, S. Hébert, D. Pelloquin, V. Hardy, A. Maignan, *Phys. Rev. B* **2006**, *73*, 165121.
[25] S. Shibasaki, W. Kobayashi, I. Terasaki, *Phys. Rev. B* **2006**, *74*, 235110.
[26] W. Kobayashi, S. Hébert, D. Pelloquin, O. Perez, A. Maignan, *Phys. Rev. B* **2007**, *76*, 245102.
[27] S. Shibasaki, I. Terasaki, E. Nishibori, H. Sawa, J. Lybeck, H. Yamauchi, M. Karppinen, *Phys. Rev. B* **2011**, *83*, 094405.
[28] S. Shibasaki, T. Nakano, I. Terasaki, K. Yubuta, T. Kajitani, *J. Phys. Condens. Matter* **2010**, *22*, 115603.
[29] R. Okazaki, Y. Nishina, Y. Yasui, S. Shibasaki, I. Terasaki, *Phys. Rev. B* **2011**, *84*, 075110.
[30] T. Motohashi, Y. Sugimoto, Y. Masubuchi, T. Sasagawa, W. Koshibae, T. Tohyama, H. Yamauchi, S. Kikkawa, *Phys. Rev. B* **2011**, *83*, 195128.
[31] A. Mendiboure, H. Eickenbusch, R. Schollhorn, *J. Solid State Chem.* **1987**, *71*, 19.
[32] A. Varela, M. Parras, J. M. González-Calbet, *Eur. J. Inorg. Chem.* **2005**, *2005*, 4410.
[33] S. Okada, I. Terasaki, *Jpn. J. Appl. Phys.* **2005**, *44*, 1834.
[34] S. Okada, I. Terasaki, H. Okabe, M. Matoba, *J. Phys. Soc. Jpn.* **2005**, *74*, 1525.
[35] Y. Okamoto, M. Nohara, F. Sakai, H. Takagi, *J. Phys. Soc. Jpn.* **2006**, *75*, 023704.
[36] P. Blaha, K. Schwarz, G. Madsen, D. Kvasicka, J. Luitz, WIEN2k, An Augmented Plane Wave + Local Orbitals Program for Calculating Crystal Properties, TU Vienna, Vienna 2001.
[37] U. Schwingenschlögl, C. Schuster, *Phys. Rev. Lett.* **2007**, *99*, 237206; *EPL* **2007**, *79*, 27003.
[38] U. Schwingenschlögl, C. Schuster, R. Frésard, *EPL* **2008**, *81*, 27002; *EPL* **2009**, *88*, 67008.
[39] N. Singh, U. Schwingenschlögl, *Chem. Phys. Lett.* **2011**, *508*, 29.
[40] G. K. H. Madsen, K. Schwarz, P. Blaha, D. J. Singh, *Phys. Rev. B* **2003**, *68*, 125212.
[41] G. K. H. Madsen, D. J. Singh, *Comput. Phys. Commun.* **2006**, *175*, 67.

[42] K. Yubuta, S. Shibasaki, I. Terasaki, T. Kajitani, *Philos. Mag.* **2009**, *89*, 2813.
[43] A. L. Hector, W. Levason, M. T. Weller, *Eur. J. Solid State Inorg. Chem.* **1998**, *35*, 679.
[44] Y. Okamoto, M. Nohara, F. Akai, H. Takagi, *J. Phys. Soc. Jap.* **2006**, *75*, 023704.
[45] K.-W. Lee, J. Kuneš, R. T. Scalettar, W. E. Pickett, *Phys. Rev. B* **2007**, *76*, 144513.
[46] K. Knížek, J. Hejtmánek, M. Maryško, E. Šantavá, Z. Jirák, J. Buršík, K. Kirakci, P. Beran, *J. Solid State Chem.* **2011**, *184*, 2231.
[47] S. Park, K. Kang, W. Si, W. S. Yoon, Y. Lee, A. R. Moodenbaugh, L. H. Lewis, T. Vogt, *Solid State Commun.* **2005**, *135*, 51.
[48] L. Viciu, J. W. G. Bos, H. W. Zandbergen, Q. Huang, M. L. Foo, S. Ishiwata, A. P. Ramirez, M. Lee, N. P. Ong, R. J. Cava, *Phys. Rev B* **2006**, *73*, 174104.